Delft University of Technology

Traffic Flow Impacts of Converting an HOV Lane Into a Dedicated CACC Lane on a Freeway Corridor

Xiao, Lin; Wang, Meng; van Arem, Bart

Important note
To cite this publication, please use the final published version (if applicable).
Please check the document version above.

Traffic Flow Impacts of Converting an HOV Lane Into a Dedicated CACC Lane on a Freeway Corridor

Lin Xiao* and Meng Wang, Member, *IEEE*
Bart van Arem, *Senior Member*, IEEE.
are with the Department of Transport and Planning, Delft University of Technology,
2600 GA Delft, The Netherlands.
E-mail: lin.xiao@tudelft.nl, m.wang@tudelft.nl, b.vanarem@tudelft.nl.

*Abstract—*Cooperative Adaptive Cruise Control (CACC) systems can increase roadway capacity, but the benefits are marginal at low market penetration rates (MPRs). Thus, a CACC dedicated lane is considered to group CACC vehicles for efficient traffic stream. Concepts of converting existing High Occupancy Vehicle (HOV) lanes into CACC lanes emerge, which leverages the infrastructural facilities and experience with HOV lanes. However, it is unclear to which extent changing HOV lanes to CACC lanes can influence freeway operations. This study examines the traffic flow impacts of converting HOV lanes into CACC lanes regarding CACC MPRs on a complex freeway corridor with multiple interacting bottlenecks in California. A simulation model capable of reproducing flow characteristics with HOV lane and CACC systems is employed for the assessment. Special attention is paid to macroscopic congestion patterns, CACC lane utilization, travel time reliability and CACC operation characteristics. The results show that converting to CACC lanes at low MPRs (<30%) can exacerbate congestion in general purpose lanes, whereas at mediate CACC MPRs (40%–50%) the congestion is drastically alleviated due to a large share of traffic carried by CACC lanes.

*Corresponding author

I. Introduction

AUTOMATED vehicles (AV) may bring fundamental changes to the traffic flow characteristics and congestion problems we are facing today [1]. In recent years, Cooperative Adaptive Cruise Control (CACC) systems that enable an equipped vehicle to maintain a small time gap to its predecessor automatically with Vehicle-Vehicle (V2V) communication, have developed fast and attracted considerable attention [2].

In the presence of CACC vehicles, traffic flow features will change since the vehicle behavior under CACC is different from that under human driver control. The impact of CACC vehicles needs to be carefully investigated before they are deployed widely in real traffic. There has been a variety of studies taking efforts to investigate the impacts of CACC vehicles on roadway capacity. Several studies [3]–[6] used analytical approaches to conclude that the capacity increase can be considerable by the reduced time gaps between two vehicles. A group of studies based on macroscopic simulations, where the traffic dynamics are taken into account, show that CACC vehicles not only increase the dynamic equilibrium capacity but also the flow stability [7]–[9]. Another group of studies assess the impacts of CACC vehicles via microscopic traffic simulations, in which the individual dynamic behavior of CACC vehicles can be explicitly modelled. The effects in increasing capacity/throughput of CACC vehicles were confirmed [10]–[17] and a quadratic relationship is found between roadway capacity and CACC market penetration rates (MPRs) [10], [11]. The capacity increase at high CACC MPRs is significant; however, the increase in capacity at low CACC MPRs is marginal [15], [16] due to the low probability of forming CACC strings in an ad-hoc way [18] or even negative if a conservative time gap is in use [14]. In this regard, a dedicated lane for CACC vehicles has been proposed as one of the solutions to facilitate the clustering of CACC vehicles and enhance the CACC string operation.

Existing studies regarding a special lane for CACC vehicles can be categorized into two groups. The studies in the first group assume an exclusive CACC lane allowing only CACC vehicles to travel in that lane. A simulation study [16] showed that a CACC lane contributes to higher throughput and speed at a lane-drop bottleneck when the MPR of CACC vehicles is more than 40%. Focusing on a merging bottleneck, the simulation in [19] showed that a dedicated lane for autonomous vehicles (using CACC algorithms) mitigated congestion and reduced scatters in the fundamental diagram when MPR is above 30%. Another recent simulation study [20] demonstrated that both the pipeline capacity and merging capacity increase by deploying a CACC lane at 40% and 60% CACC MPRs. These three studies pointed out that the effectiveness of CACC lanes is highly related to the CACC market penetration rate, being consistent with the findings of an analytical study regarding the deploy-

ment of an AV lane [21]. However, study [16] focused on a single lane-drop bottleneck without on/off ramps, where the impacts of CACC vehicles' lane changes in preparation for entering CACC lanes and exiting highway are neglected; and the simulations of the hypothetical merging segments and the real multi-ramp network in [19] and [20] do not provide a realistic and reliable estimation of CACC vehicle impacts in a traffic corridor level. The simulated real network in [19] is too short (less than 6 km) to fairly show the CACC benefits for a multi-ramp corridor because the actual travelling distance by CACC in dedicated lanes might not be sufficient to reveal substantial benefits. The simulation of the SR99 corridor in [20] only investigated the impacts of CACC vehicles with a combined strategy of a CACC lane and connected vehicles at the 20% CACC level. The impacts of only deploying CACC lanes at other CACC MPRs are not specified.

Instead of assuming exclusive CACC lanes, the second group of studies assume CACC vehicles can access existing dedicated lanes, e.g. high occupancy vehicle (HOV) lanes. In [22], 20% of overall traffic with CACC vehicles were assigned in the HOV lane in addition to 10% of overall traffic with HOVs. This results in a higher throughput but a lower average speed at high traffic demands, compared to the cases of 0% CACC and 20% CACC vehicles travelling across all the lanes without a dedicated lane. In [23] a tolling discount for CACC vehicles travelling in a tolling HOV lane is assumed in the lane choice model during dynamic traffic assignment. It is concluded that opening the HOV lane for CACC vehicles is not beneficial for increasing the use of HOV lanes and bottleneck speeds at 20% CACC MPRs, but it is beneficial at 60%–100% CACC MPRs. In both studies, no lane change activity was taken into account for CACC vehicles so the concluded impacts are more related to the steady-state operations of barrier-separated HOV lanes.

Beyond the categorization, a study [24] discussed the optimal lane deployments in terms of roadway capacity in equilibrium states, from the aspects of mixed-used or separated-used lanes for regular vehicles and AVs. At low MPRs, the optimum capacity is achieved when all lanes are mixed-used lanes and all AVs are allocated only in one of them; at high MPRs, the optimum lane deployment will be a combination of a separated-used lane for AVs and mixed-used lanes for regular vehicles. However, from the aspect of CACC vehicle strings operation, the presence of regular vehicles can easily cause string separations and CACC degradations to ACC. Thus a mixed-used lane is not ideal to cluster CACC vehicles for string operation. In this study, we focus on the exclusive lane for CACC vehicles, termed CACC lanes.

Overall, the literature pointed out that the traffic impacts of a CACC lane are complex, and correlate with traffic demand and CACC MPRs. Although the literature has shown that a CACC lane can increase throughput/capacity

and alleviate congestion at either a lane-drop or a merging bottleneck, those benefits are generally overestimated when it is discussed at a realistic corridor due to the negative influence by the additional lane changes of CACC vehicles from on/off ramps. The combined effects of a CACC lane and CACC MPRs at a corridor with multiple interacting bottlenecks have not been addressed, and the question of how to deploy CACC dedicated lanes is still challenging to road operators, especially whether it is beneficial to leverage existing HOV lanes to encourage early deployment of CACC. In this regard, this research investigates the traffic impacts of converting an HOV lane into a CACC lane and reveals the effects of a CACC lane at different CACC MPRs on congestion pattern, travel time reliability and CACC system operation at a highway corridor. We select a realistic traffic corridor with an HOV lane as the reference case and identify at which CACC MPRs it is beneficial to convert an HOV lane to a CACC lane.

The main contribution of this study is to offer new insights into the corridor-level impacts of converting an exclusive HOV lane to an exclusive CACC lane at various MPRs as distinguished from a single bottleneck [16], [18]–[20]. The simulated network is sufficiently large to show the benefits of CACC operation on long-distance trips. The network involving various merging, diverging, and weaving sections is able to generate realistic traffic disturbances and nonlinear traffic flow phenomena on a corridor with interacting bottlenecks. The ratio between the dedicated lane and the general purpose lanes varies along the corridor and the dedicated lane is activated and de-activated during the simulation, which captures the additional lane changes of CACC vehicles due to the presence of the dedicated lane. In addition, the simulation model captures the CACC operational characteristics and driver-automation interaction. Thus, the trade-off between the positive effects of the CACC lane in clustering CACC vehicles and the negative effects of inducing more lane changes and more CACC deactivations can be evaluated in this unique simulation framework.

The paper is structured as follows. Section 2 introduces the car-following model for CACC vehicles and conventional vehicles in our simulation and the lane change model particularly applied to the continuous-access dedicated lane scenario. Section 3 elaborates the simulation experiment design and set-up to explore the impacts of CACC MPRs in a scenario with a CACC dedicated lane. After that, simulation results are presented and discussed in the fourth section, followed by the conclusion and future work in Section 5.

II. Car-following and Lane Change Models for Microscopic Simulations
This section summarizes the vehicle behavioral models proposed in our previous studies [25], [26] for CACC vehicles and manually driven vehicles in microscopic simulations. A framework for integrated lane change and car-following model is presented, followed by brief descriptions of CACC and manually driving car-following model, as well as the lane change model for dedicated lane scenarios.

A. Framework for Integrated Lane Change and Car-following Model
Fig 1 shows the framework of how the lane change model and car-following model are integrated with the hierarchical structure of driving tasks. The lane change model is placed at the tactical level, where drivers make the decisions for lane change and gap acceptance; the car-following model is located at the operational level, where acceleration models are executed. The outputs of the lane change model are used as the inputs of car-following models.

The possible outputs from the lane change model are three lane change intentions: *stay in the lane*, *lane change preparation* and *change lane to left or right*. The *stay in the lane* is the result of either no lane change desire shows up or the gap for a free lane change is rejected. The decision of *change lane to left or right* is made when lane change desire is larger than a minimum value and the gap is acceptable. The *lane change preparation* occurs only when a lane change decision has been made with large desires but the current gap is unacceptable. The vehicle has to adjust its car-following behavior or request cooperation from other vehicles to conduct the lane change.

The three different lane change intentions determine different paths to choose between the CACC and the manually driving car-following models at the operational level. Following the intention of *stay in the lane*, CACC vehicles can be activated or deactivated by the driver. In the *lane change preparation*, CACC will be deactivated and the manually driving model will be the only option because the preparation behavior is only assumed to be conducted by human drivers. During the lane change execution, no switch between CACC and manual driving is allowed. Therefore, the dominating car-following model remains as it is. After the execution of car-following models, the time moves to the next time step. This set of the hierarchically integrated lane change and car-following models represent the driving behavior of a CACC vehicle in both lateral and longitudinal response.

B. Car-following models under CACC

1. Car-following models in three operation modes
The ACC and CACC controllers consist of three modes for three different control objectives [27]–[29]. The cruising mode is designed to maintain a user-set desired speed if a preceding vehicle is out of detection range or faster than the subject vehicle's desired speed; the gap-regulating mode works for the car-following situation and aims to
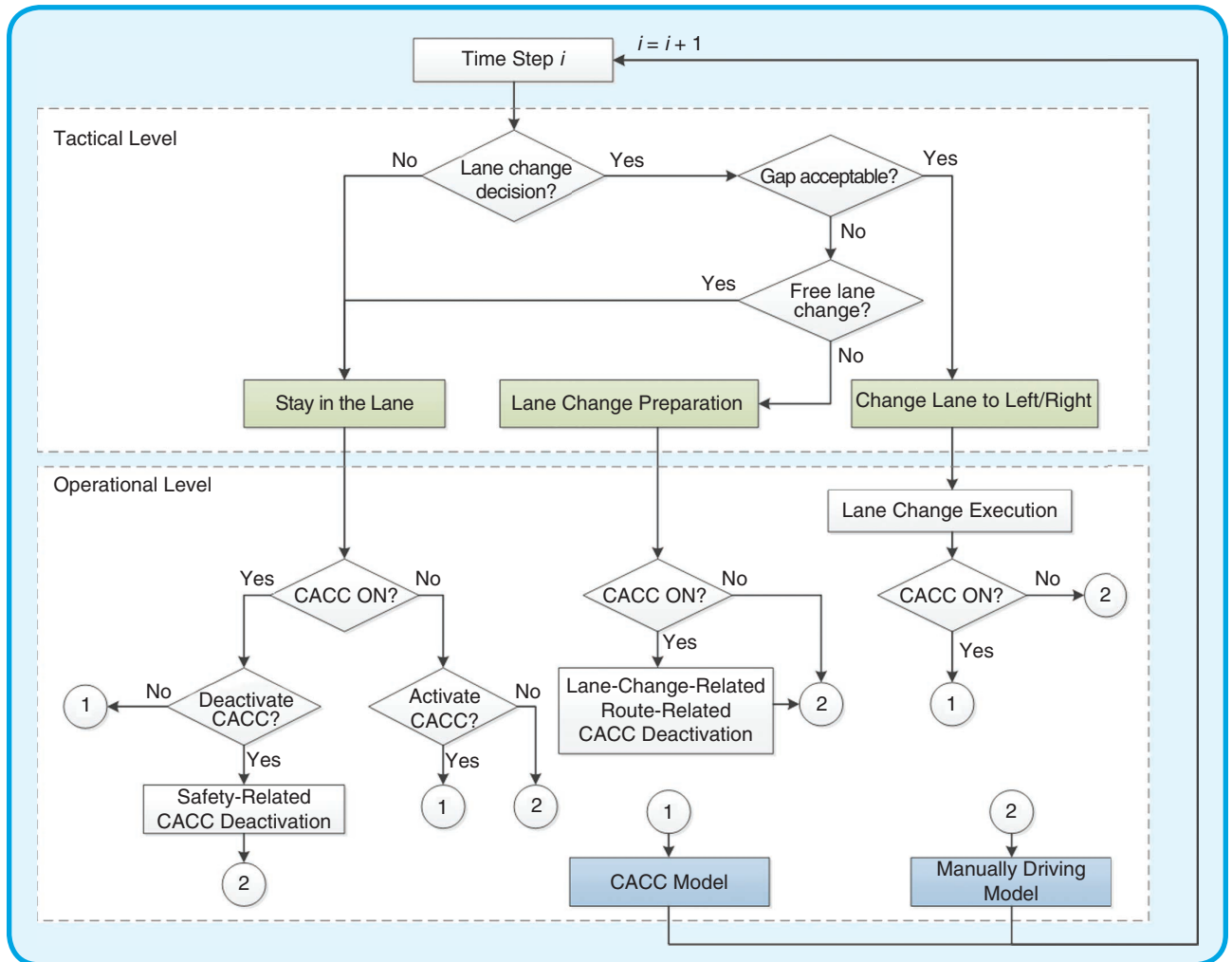
FIG 1 Framework for the integrated lane change and car-following model.

maintain a constant time gap with its predecessor. The gap-closing mode performs a transition from the cruising controller to the gap-regulating controller when an ACC/CACC approaches its leader from a long range.

Each mode has its own car-following model as formulated in Table 1. The ACC and CACC systems share the same model for the cruising mode since the V2V communication does not play a role when the vehicle is only targeting the desired speed. The gap-regulating mode and gap-closing mode also have the same model structure, whereas the control gains in different modes vary. For a detailed specification of the models, we refer to [26].

The desired speed and desired following time gap are the model inputs. We assume the same desired speed under ACC/CACC as it is under the manually driving, and the desired time gap follows a realistic distribution of time gap setting collected from a field test [30]. The maximum CACC string length is 10 vehicles and the minimum desired time gap between two strings (inter-string gap) is assumed to be 1.5 seconds [31].

Table 1. MODEL SPECIFICATIONS FOR THREE OPERATION MODES UNDER ACC AND CACC

Driving modes	Model specifications
ACC Cruising	$a_{i,k} = 0.4 \cdot (v_{des} - v_{i,k-1})$
ACC Gap-regulating	$a_{i,k} = 0.23 \cdot e_{i,k} + 0.07 \cdot (v_{i-1,k-1} - v_{i,k-1})$
ACC Gap-closing	$a_{i,k} = 0.04 \cdot e_{i,k} + 0.8 \cdot (v_{i-1,k-1} - v_{i,k-1})$
CACC Cruising	$a_{i,k} = 0.4 \cdot (v_{des} - v_{i,k-1})$
CACC Gap-regulating	$v_{i,k} = v_{i,k-1} + 0.45 \cdot e_{i,k-1} + 0.0125 \cdot d(e_{i,k-1})/dk$
CACC Gap-closing	$v_{i,k} = v_{i,k-1} + 0.005 \cdot e_{i,k-1} + 0.05 \cdot d(e_{i,k-1})/dk$
	$e_{i,k} = x_{i-1,k-1} - x_{i,k-1} - t_{des} \cdot v_{i,k-1} - d_0$

Note: i is the vehicle sequence; k is the simulation time step; a, v and e are the vehicle acceleration (m/s^2), speed (m/s) and gap error (m); v_{des} is the desired speed (m/s); t_{des} is the desired time gap (s) and d_0 is a dynamic spacing margin (m) proposed in [26].

2. Automation system activation and deactivation

System activation and deactivation, as driver's interaction with the automation system, specify the switching logic

between the CACC and manually driving car-following models. In this study, system activation is based on the assumption that drivers intend to use the ACC/CACC system as much as possible. Thus, the ACC/CACC will be switched on as long as the operational design domain allows. In two situations the ACC/CACC system will not be activated: the vehicle is braking over 2 m/s^2 and the vehicle is performing a lane change.

There are three types of system deactivation and there is a minimum time period of remaining deactivated to avoid frequent deactivation within a short time period. The first type of system deactivation is safety-related, including the system-initiated deactivation and the driver-initiated deactivation for avoiding rear-end collisions. From the system-initiated aspect, a collision warning based on inverse time-to-collision [32] is employed to identify safety-critical situations and inform the driver to take over vehicle control. The ACC/CACC system is allowed to be re-activated 5 seconds after the collision warning is not issued. In addition, drivers are also assumed to actively resume vehicle control in a high-relative-speed approach scenario, and re-activation is possible 10 seconds after the deactivation criterion is not satisfied. The second type of system deactivation is related to lane change behavior, in particular when drivers need to synchronize their speeds for a lane change or create a gap in front to facilitate a vehicle to merge. Drivers override systems to conduct such lane change preparations and once the lane change is completed, CACC is reactivated in 2 seconds. This type of deactivation highly depends on the lane change desire, which will be explicitly explained in the following lane change model section. The last type of deactivation is related to the route. It is assumed that when vehicles have to make mandatory lane changes to follow a particular route, drivers will resume control until the vehicle arrives the target lane to avoid the frequent switch between automation and human-driven system.

C. Car-following model under manual driving

The car-following model for human drivers is a modified version of the Intelligent Driver Model [33], referred as IDM+ [34]. The behavioral assumption behind the IDM and IDM+ is that in unconstrained driving conditions drivers regulate vehicle accelerations towards the free/desired speed and in constrained driving conditions drivers control acceleration to follow the predecessor in a safe and comfortable way. The IDM+ outputs the vehicle acceleration as the minimum of the acceleration of driving towards the desired speed and the acceleration towards the desired headway. It is formulated as

$$\dot{v} = a \cdot \min(1 - (v/v_{\text{des}})^4, 1 - (s^*/s)^2) \quad (1)$$

and

$$s^* = s_0 + v \cdot T + v \cdot \Delta v / 2\sqrt{a \cdot b} \quad (2)$$

where a, b are the maximum acceleration and comfortable deceleration in m/s^2, v_{des} is vehicle's desired speed in m/s, and s^* is the dynamic desired distance headway in the meter. T and s are the time gap in second and distance gap in meter, whereas the s_0 is the stopping distance and Δv is the approaching rate to a leader in m/s. The IDM+ is able to generate more reasonable capacity values compared to the IDM.

The time gap is relaxed between a minimum time gap $T_{\min}$ at a maximum lane change desire and an equilibrium following time gap $T_{\max}$ which is defined as a constant value during the entire simulation period. However, to simulate a long road network which has complex road configurations such as varying lane numbers and multiple types of bottlenecks, a constant $T_{\max}$ is not adequate to depict the characteristics of driving behavior adapted to different road configurations. Thus, we introduce a location-based fraction of $T_{\max}$ for better reproduction of traffic flows, e.g. roadway capacity, and the fractions are to be calibrated in each case study.

D. Lane change model for dedicated lane operation

The lane change model, for both CACC and manually driven vehicles, is based on the Lane Change Model with Relaxation and Synchronization (LMRS) in [35]. In order to model the adapted vehicle behavior with the presence of dedicated lanes, we extended this model for eligible users and ineligible users in terms of the accessibility to dedicated lanes.

1. Basic LMRS

The lane change model postulates that a drivers' lane change desires consist of incentives to follow the right route to the destination (mandatory lane changes), to maintain or gain speed, and to comply with traffic rules. The LMRS calculates the lane change desire to decide whether to change lane and what type of lane change is needed. This is followed by a gap acceptance model to determine if the available gap is acceptable at the current desire level. The route incentive is a mandatory lane change incentive, which arises if the current lane will not allow a vehicle to follow its route. It is determined either by the remaining distance or by the remaining anticipated travel time to the target lane that can continue to follow the route. A driver's desire to change lane for higher anticipated speed is defined as the speed incentive. It is expressed as a function of the anticipated speed gain from the target lane. The directional bias is applied in accordance with the keep-right traffic rule, which is implemented as a constant bias to the right lane. The speed incentive and directional bias are discretionary lane change incentives, which are only partially included when the route incentive appears. The model is generally formulated as

$$d^{ij} = d_r^{ij} + \theta^{ij} \cdot (d_s^{ij} + d_b^{ij}) \quad (3)$$

where d^{ij} is the overall lane change desire from lane i to lane j. d_r^{ij}, d_s^{ij} and d_b^{ij} represent the incentives for the route, speed and a directional bias respectively, and θ^{ij} is a weight factor reflecting the relative importance of discretionary incentives.

Four types of lane change behavior are specified according to the overall lane change desire, being No Lane Change (No LC), free lane changes (FLC), synchronized lane changes (SLC) and cooperative lane changes (CLC). The relationships between lane change desire and resulting lane change behavior are shown in Fig 2 with behavioral changes in synchronization and gap-creation. The synchronization refers to the speed synchronization of the lane changer to its target leader, and the gap-creation refers to the courtesy behavior of the potential follower in the target lane to facilitate the lane change. As lane change desire increases, lane changing vehicles first intend to perform the FLC without additional strategies. As lane change desire falls into the SLC range, a lane-changing vehicle aligns its speed with that of the leader in the target lane, but the follower in the target lane does not actively create a gap for the lane changer. When the desire exceeds the CLC criteria, cooperative lane changes (CLC) are expected, in which the lane-changing vehicle synchronizes its speed with the potential leader in the target lane and the potential follower in target lane also actively creates a gap in front for the lane changer.

In addition, the interaction between the lateral and longitudinal vehicle behavior is modelled by expressing the acceptable gap and acceleration level as linear functions of the lane change desire. As lane change desire increases, the acceptable headway decreases and the acceptable deceleration increases, both of which increase the likelihood of successful lane changes. The mathematical formulation of the interaction can be found in reference [35].

2. Eligible users to a dedicated lane

Speed incentive and lane preference are two lane change incentives toward dedicated lanes taken into account by eligible users. The speed incentive for gaining speed on an adjacent dedicated lane has been captured by the original LMRS, whereas for users travelling on general purpose (GP) lanes that are further away from the dedicated lanes, the speed incentives are indirectly captured by an accumulated adjacent speed gain in each lane change process. The lane preference on the dedicated lane by eligible users is considered as a particular direction bias of lane changes, i.e. to-left or to-right. This direction bias will increase the lane change desire toward dedicated lanes and it works
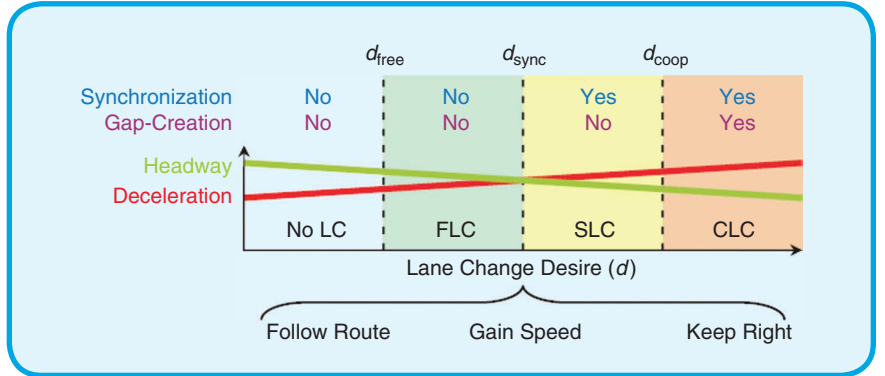

FIG 2 Four types of lane change behavior corresponding to the level of lane change desire [35].

during multiple lanes changes until a vehicle has arrived at the dedicated lanes.

A direction bias toward a dedicated lane (DL), denoted as d_{DL}^{ij}, is proposed in the LMRS framework as a discretionary incentive. The lane change desire of eligible users is thus formulated as (4), where the keep-right bias in the original model is removed because the keep-right rule does not apply in the simulated U.S. traffic.

$$d^{ij} = \begin{cases} d_r^{ij} + \theta^{ij}(d_s^{ij} + d_{DL}^{ij}) & \text{head for DL;} \\ d_r^{i,j} + \theta^{i,j} \cdot d_s^{i,j} & \text{otherwise.} \end{cases} \quad (4)$$

3. Ineligible users to a dedicated lane

Ineligible users are obliged to leave the dedicated lanes when the dedicated lane is activated. They may leave the dedicated lane immediately or gradually if sufficient gaps in the adjacent GP lanes are not found. Such egressing behavior can be modelled by a directional bias d_{leave}^{ij} to the direction of the adjacent GP lane. This bias increases the lane change desire of going to the adjacent GP lane and generally leads to a relatively active lane change behavior, e.g. the SLC and CLC. Once the ineligible users have left the dedicated lanes, their desire toward dedicated lanes becomes infinitely negative, indicating that they will not change back to dedicated lanes. The lane change desire of ineligible users to a dedicated lane is expressed in (5).

$$d^{ij} = \begin{cases} d_r^{ij} + \theta^{ij}(d_s^{ij} + d_{leave}^{ij}) & \text{leaving DL;} \\ -Inf & j \text{ is a DL;} \\ d_r^{ij} + \theta^{ij} \cdot d_s^{ij} & \text{otherwise.} \end{cases} \quad (5)$$

This completes the description of the car-following model and lane change model for simulated CACC vehicles and manually driven vehicles in our study. This integrated model outperforms the other CACC simulation models for its capability in reproducing realistic CACC vehicle behavior in simulations. It models the multi-mode operation of the CACC system and the interaction between the driver and the system, describing extensively the CACC vehicle states on road. The manually driving behavior including

the lane change behavior adapted to dedicated lanes is explicitly modelled and properly calibrated. In the following section, the experiment and simulation set-up for determining the traffic impacts of a CACC lane will be provided.

III. Experimental setup

To investigate the impacts of CACC vehicles on traffic flow with a dedicated CACC lane and explore the interaction between CACC MPRs and a dedicated lane deployment, we conduct simulation experiments by introducing CACC vehicles and a left-most CACC lane in a realistic network with interacting bottlenecks.

The SR-99 corridor to the south of Sacramental in California is chosen as the simulation network. The corridor is 20-km long with 16 on-ramps, 12 off-ramps and 1 High Occupancy Vehicle (HOV) lane, heading from the Elk Grove Blvd to the interchange for SR-50. The number of lane increases from three lanes to four lanes at the merge of Calvine Rd and further increase to five lanes after the interchange with Fruitridge Rd. The leftmost lane is a continuous-access HOV lane, where eligible vehicles are free to enter and exit at any location. In the morning, it is only activated during 6:00–10:00 AM. Fig 3 presents the lane configuration with lane-based loop detectors. In total, there are 16 reliable groups of detectors illustrated as rectangles with their post miles. The 5-min flow and speed provided by these detectors exhibit the traffic flow performance in this corridor, in which there is recurrent congestion in the morning peak contributed by three interacting bottlenecks: the merging section at Sheldon Rd., the weaving section at Florin Rd. and 47th Ave. Our simulation starts from 4:00 AM to 12:00 AM, covering the operations of free flows, traffic breakdown and congestion recovery, as well as the inactive and active periods of the HOV lanes.

The selected network and scenario were established in an open-source microscopic traffic simulator, MOTUS [36], where the basic LMRS and IDM+ are adopted and integrated. The lane change model has been extended in our previous work [25] to model dedicated lane operations and the car-following and lane change models for CACC vehicles have been implemented in the simulator [18]. In the previous study [25], we have calibrated the manually driving car-following model and lane change model using the loop detector data of October 6, 2015 from the Caltrans Performance Measurement System (PeMS), which is chosen for a typical weekday without incident reports during the simulated time period. Four parameters in the IDM+ and nine parameters in the extended LMRS were calibrated and the models are able to reproduce plausible vehicle behavior and replicate a consistent congestion pattern, fundamental diagrams and lane flow distribution at network, section and lane level respectively with the PeMS data. The calibrated simulation is taken as the reference case for comparison with simulations of CACC vehicles in a CACC dedicated lane scenario.

In this experiment, we replace the HOV lane by a CACC lane. Similar to the HOV lanes, the CACC lane is only accessible to CACC vehicles once activated, but CACC vehicles can travel in all lanes. All the other simulation settings and parameters (see Table 2) remain unchanged except for a percentage of passenger cars changing into CACC vehicles. The truck percentage remains at 3.8% of all traffic, an average of truck flow over the mainline flow in this corridor. We use the largely time-variant demand pattern from the reference case and assume an invariant generated CACC percentage during the simulation period.

When a CACC dedicated lane is activated, the vehicles generated at that lane should only be CACC vehicles, instead of mixed vehicle types to avoid mandatory lane changes at the network beginning due to lane accessibility. In order to meet this requirement while ensuring CACC market penetration rate is respected as the simulation input, we distribute the mainline demand to the three mainline generators so that when the dedicated CACC lane is activated, only CACC vehicles are generated in this lane.

The simulated CACC vehicle percentages increase from 10% to 50% by an increment of 10%, and each CACC MPR is run five times with different random seeds. For the impacts of CACC vehicles on traffic congestion, the spatiotemporal speed contour of the corridor is plotted for the identification of the changes in congestion pattern. The congestion pattern is further explored with CACC lane operation and friction effects, which can be analyzed via CACC lane throughput and speed. In addition, changes
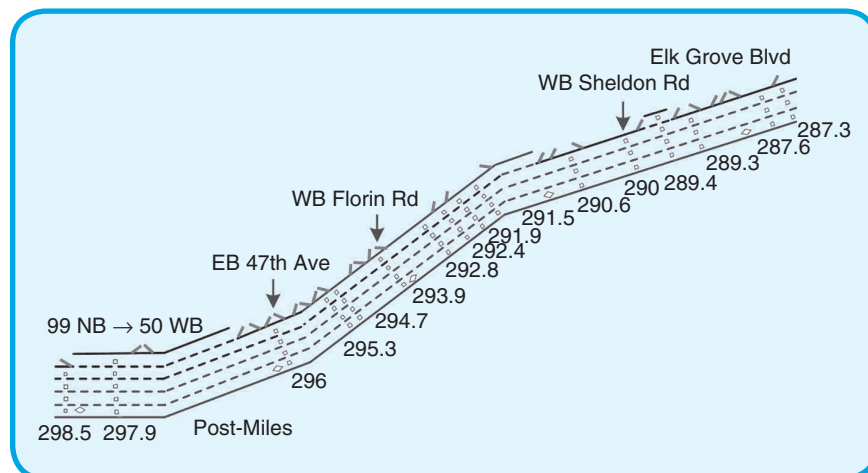
FIG 3 Lane configuration and road geometry of the SR-99 corridor.

in travel time reliability in each CACC MPR scenario are investigated and statistics on CACC time usage and number of deactivations are provided to show the operation of CACC strings. It takes on average 24 minutes to run one scenario of 7 hours with MOTUS.

IV. Simulation Results

This section presents the simulation results with increasing CACC vehicle MPRs in terms of the macroscopic congestion pattern, the utilization of CACC dedicated lane, travel time reliability and CACC system operations. The analysis of congestion pattern and CACC lane utilization are carried out from the traffic flow perspective, whereas the discussions on travel time reliability and CACC operations are mainly at the platoon and vehicle/driver levels.

A. Traffic congestion pattern

Fig 4 shows the macroscopic flow operations with CACC MPRs via the speed plot in the time-space diagram. From 10% to 50% MPRs, the congested area at 10%–20% CACC MPRs is considerably large, then becomes small at 30% and further substantially reduces to a small area after 40% CACC MPRs. It depicts a general trend of alleviated congestion with increasing CACC MPR in the network. Compared to the reference case, a low CACC MPR with a CACC lane does not show positive impacts in reducing congestion. The congestion area at 10% and 20% CACC percentage is much larger than the reference case and at 30% MPRs the congestion area is just comparable to the reference case. The HOV ratio in the reference case is time-variant and the averaged HOV ratio is around 29% during 6:00–8:00 AM when the traffic congestion emerged and propagated in the network. The comparable vehicle percentages eligible for the dedicated lane in reference case and 30% CACC case can explain the similar congestion pattern in both cases and it suggests that the formation of congestions at 10%–30% CACC MPRs is mainly caused by closing one lane for manually driven vehicles whereas there is insufficient flow on the CACC lane. These results imply that the potential improvements by CACC vehicles are offset by the underutilization of a CACC lane at low MPRs.

Looking into the characteristics of traffic congestion, increasing the CACC MPR does not change the location of a bottleneck in the network. In Fig 4, it is clear to observe the activated bottlenecks at Sheldon Rd. (PM 290.0), Florin Rd. (PM 293.9) and 47th Ave (PM 296.0) at 10–30% CACC MPRs, which also are the bottlenecks identified in the reference case. However, increasing CACC MPRs delays the onset of congestion, especially for the Shelden bottleneck. The congestion starts at 6:40 AM in the reference case and at 6:20, 6:45 and 7:05 AM at 10%, 20% and 30% MPRs respectively. After the 40% MPRs, the congestion at this bottleneck is entirely prevented, given the same demand as the reference case.

Table 2. EMPLOYED PARAMETERS IN SIMULATION	
Parameters	Typical value
Car-following model	
Conventional vehicles	
Maximum acceleration	1.25 m/s^2
Comfortable deceleration	2.09 m/s^2
Stopping distance	3 m
Shared with conventional vehicles and CACC vehicles	
Desired time gap under manual driving	1.4 s
Vehicle length	4 m
Free-flow speeds	N(125, 8.75) km/h
CACC vehicles	
V2V communication range	300 m
Sensor range	120 m
Desired time gap under ACC	1.1 s
Desired time gap under CACC	0.6 s (57%), 0.7 s (24%) 0.9 s (7%), 1.1 s (12%)
CACC inter-string gap	1.5 s
CACC string length limit	10 vehicles
ACC-CACC lower acceleration limit	–4 m/s^2
ACC-CACC upper acceleration limit	2 m/s^2
Lane change model	
Free lane change criteria	0.25
Synchronized lane change criteria	0.5
Cooperative lane change criteria	0.75
Bias to head toward dedicated lanes	0.45
Bias to leave the dedicated lane	0.5

With the same demand setting for each scenario, the delayed timings for the onset of congestion suggest the potential of CACC vehicles, in combination with a CACC lane, in postponing or preventing traffic congestion. A CACC lane provides high vehicle throughput. When there is sufficient CACC demand, a considerable amount of traffic can be shared by CACC lanes, leading to less demand in GP lanes and therefore the congestion is less likely to appear. In addition, the CACC vehicles travelling in GP lanes are able to increase the throughput of GP lanes, which also prevents or postpones traffic breakdowns.

The changes in congestion pattern also reveal that the effectiveness of converting an HOV lane to a CACC lane is highly related to the percentage of CACC vehicles in traffic. Under 30% MPR, the CACC lanes may not be able to share sufficient traffic and the CACC vehicles remaining in GP lanes are also not effective to alleviate the congestion.
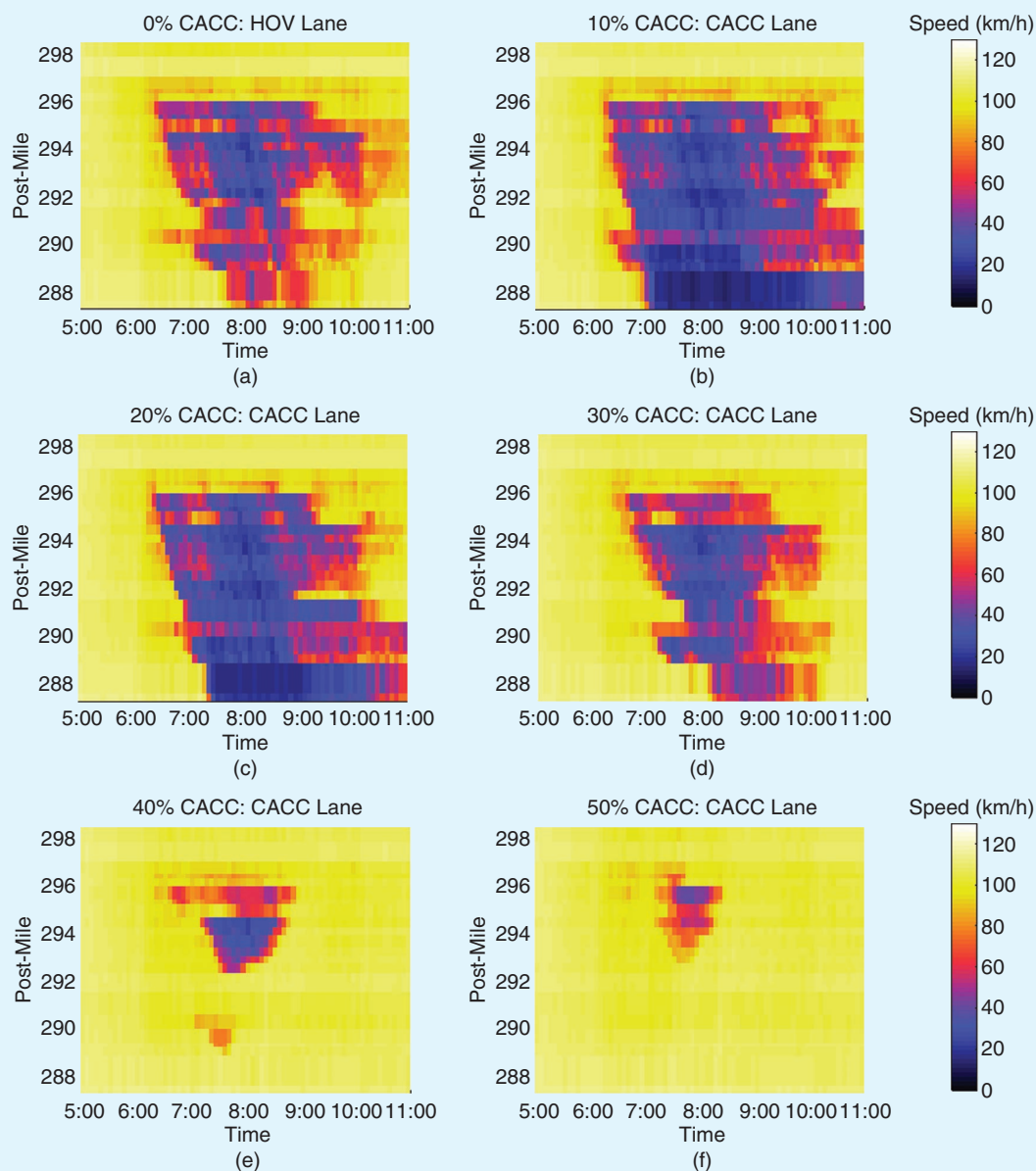
FIG 4 Traffic congestion pattern with increasing CACC MPRs in a CACC dedicated lane scenario.

B. CACC lane operation and friction effects

Fig 5 provides speed-flow plots at each bottleneck with different CACC MPRs during 6:00–7:30 AM that the congestion was formed. Firstly, the results show that the traffic volume/flow of CACC lanes increases with the CACC MPRs at each bottleneck and they are all below the lane capacity of 100% CACC vehicles which is around 3300 veh/h/lane at a merging bottleneck [18]. It implies that the traffic flow on CACC lanes is not oversaturated and CACC lanes can still carry more traffic when the overall CACC MPR is below 50%. Secondly, it is noted that sometimes the speed reduces substantially even though the flow remains at a low level. This suggests that the congestion in CACC lanes is not caused by high traffic demands but by lane changes of CACC vehicles between CACC lanes and GP lanes.

The speed reduction of dedicated lanes as a result of interacting traffic between dedicated lanes and adjacent GP lanes is described as the friction effect, and it is a general phenomenon for traffic flow with a continuous-access dedicated lane [37]. A friction effect appears before dedicated lanes reaching the capacity and corresponds to the traffic congestion in adjacent GP lanes. To understand the interaction between the CACC lanes and GP lanes, the speed reductions in both lanes are investigated.
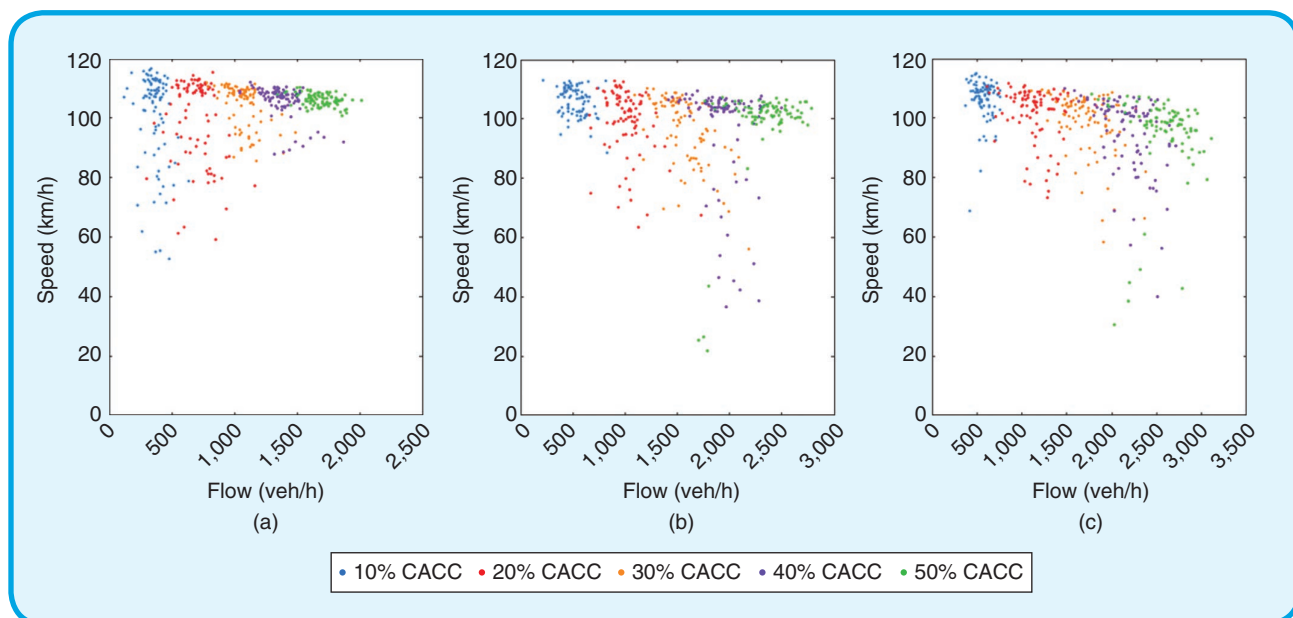
FIG 5 The speed-flow plots of the CACC lane during 6:00-7:30 AM at different CACC MPRs at three bottlenecks. (a) Shelden Rd. Bottoleneck, (b) Florins Rd. Bottoleneck, and (c) 47th Ave. Bottoleneck.

The speed contour plots of the CACC lanes and adjacent GP lanes, as well as the plots of their speed differences, are presented in Fig 6. With a CACC dedicated lane, the friction effect remains observable at all tested CACC MPRs. At low CACC MPRs 10–30%, speed reductions in the CACC lanes are observed only at several particular sections. The speed differences between CACC lane and the adjacent GP lane are considerable, reaching up to 100 km/h at some locations that can lead to adverse consequences on safety. At high CACC MPRs, the time-space area of speed reductions in the dedicated lane is more comparable to the congestion in the adjacent GP lanes and the speed difference of the congested area are relatively small. Hence, the friction effect is more significant. This is consistent with the observation in [25] that the friction effect does not occur when the demand in dedicated lanes is low.

In our model, the friction effect is mainly due to the lane change maneuvers for entering and exiting the dedicated lane which disrupts the flow on the dedicated lane [25]. With a CACC string operation in the dedicated lanes, the following gaps between two vehicles are generally smaller than that between manually driven vehicles, which makes it difficult for a CACC vehicle to merge into the CACC lane. In this case, a cooperative lane change initiated by a CACC vehicle from the adjacent GP lane, requiring the potential follower in the CACC lane to intentionally create a sufficient gap, causes severe disruption in the CACC lane. In addition, the speed reduction in the CACC lane is also caused by CACC drivers slow down to search an acceptable gap for performing a lane change toward highway exits.

C. Travel Time Reliability

The speed difference between CACC lane and GP lanes implies unequal travel time for vehicles travelling in those lanes. Table 3 provides the statistical analysis of total travel time of all vehicles and average travel time delay per vehicle regardless of vehicle classes, by which the effects of CACC lanes at each CACC MPRs are quantified. The total travel time and averaged travel time delay firstly increase from 0% to 10% CACC MPRs and later decrease with CACC MPRs, which is consistent with the traffic congestion pattern in Fig 4. At the 10% and 20% MPRs which the CACC lanes worsen the traffic performance, the increases in travel time are as high as 42% and 31%, whereas the increases in travel time delay reach 110% and 75%. At 40% and 50% MPRs where less congestion is observed, the reductions in travel time are 31% and 36% and in travel time delay are 71% and 77%, a considerably large save.

The standard deviation of averaged travel time delay shows the impact of congestion on travel time reliability. As the results presented, more severe congestion is, less reliable the travel time is. Although at 30% CACC MPRs, it seems that the congestion pattern and travel time are comparable to the reference case, the results show a larger delay and standard deviation, implying reduced travel time reliability at this MPR due to a mixture of CACC and conventional vehicles.

To distinguish the travel time reliability of CACC and conventional vehicles, Fig 7 shows their averaged travel time delay and its deviation at each MPRs separately. During the 10–30% CACC MPRs, the differences are substantial, suggesting that CACC dedicated lane does lead to less travel time delay and provide more reliable travel time to
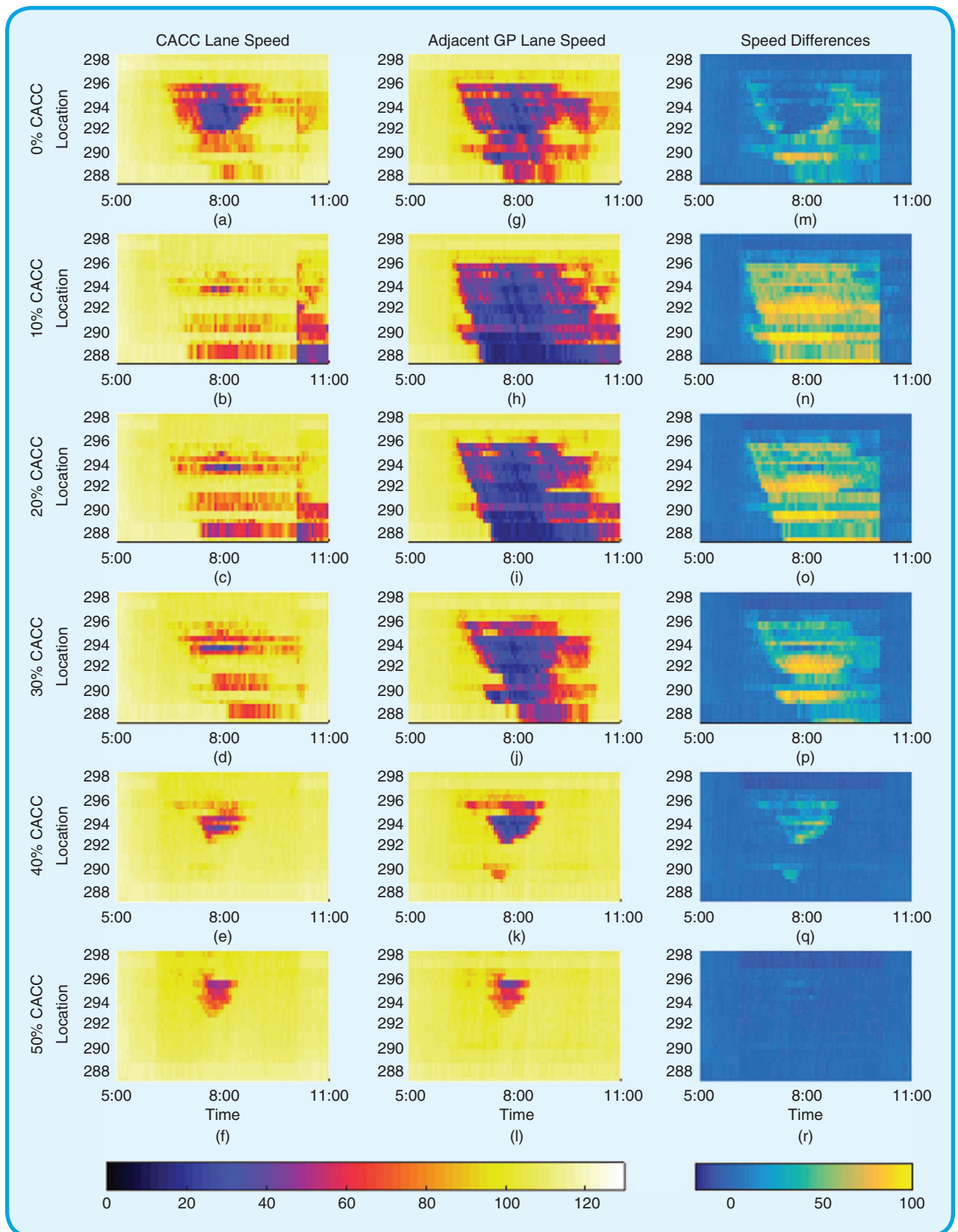
FIG 6 Speed differences of dedicated lanes and the adjacent general purpose lanes at different CACC MPRs.

CACC vehicles. At 40% CACC MPRs, although the difference in delay is insignificant, the discrepancy in variation prevails. It is explained by the light traffic jam in this scenario that the travel time will not differ much between the CACC lanes and GP lanes. However, at 50% CACC MPRs, the variation of CACC vehicles in delay is slightly higher than conventional vehicles, which might be the consequences of additional lane changes toward and egressing the dedicated lanes. These results point out the effectiveness of CACC lanes in providing shorter travel time and higher travel time reliability to CACC vehicles in saturated traffic.

D. CACC system operations

The operational characteristics of the CACC system reveal to what extent the CACC system is effectively and sufficiently used in mixed traffic. In this section, the CACC usage in each MPR scenarios is examined, illustrating the impacts of increasing MRPs on CACC operations with a presence of CACC lane.

CACC time usage is an important indicator of the operation of CACC systems. It is calculated for each CACC vehicle, based on vehicle trajectories, as the ratio of the accumulated time duration under CACC operation over the entire travel time. In Table 4, the CACC time usage increases as the percentage of CACC vehicles increases, which rises from 23.94% to 48.45%. It is explained by the increase in the probability of CACC vehicles following another CACC vehicle. Higher MPR leads to a higher probability and thus the CACC time usage increases.

Regarding string operation, the time usage under the CACC gap-regulating mode is investigated. For comparable results among different scenarios, it is calculated as the ratio of the accumulative time duration under gap-regulating mode over the time usage of CACC for each vehicle. Table 4 lists the average value of five simulation runs at each CACC MPR. The lower the CACC MPR is, the higher the ratio is. This trend is explained by the existence of a CACC dedicated lane. Since more severe congestions happen at low CACC MPRs, CACC vehicles on GP lanes have larger desires to change to the dedicated lane to gain speeds. CACC vehicles travelling in the dedicated lane experience less interference from merging and exiting traffic than that in GP lanes, therefore CACC vehicles are more likely to be operated in the CACC gap-regulating mode.

The number of CACC deactivations reflects to what extent CACC operation is interrupted and it is highly related to throughput reduction in mixed traffic flows [18]. Table 4 provides the average number of CACC deactivations per CACC vehicle and also the number in each deactivation category. In general, the number of safety-related deactivation changes significantly with the MPRs, whereas the other two categories of deactivation vary insubstantially. The safety-related deactivation decreases from around 3 per vehicle at 10–20% CACC MPRs to 1 per vehicle at 50%

Table 3. TRAVEL TIME AND DELAY ANALYSIS OF ALL TRAFFIC IN EACH CACC MPR

	CACC					
	0%	10%	20%	30%	40%	50%
Total TT (h)	10961	15546	14337	10997	7586	7065
mean TTD (s/veh)	255	536	446	324	86	79
std TTD (s/veh)	381	861	723	555	110	89

Note: TT is travel time; TTD is travel time delay and std is the standard deviation.

Table 4. CACC OPERATIONAL CHARACTERISTICS

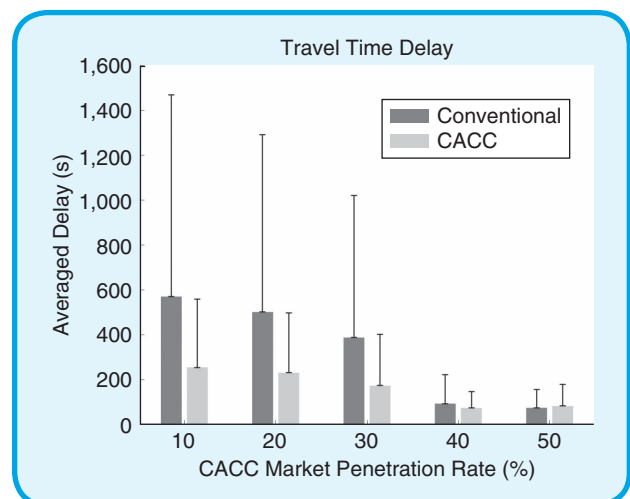|	CACC MPRs				
	10%	20%	30%	40%	50%
Time Usage per CACC vehicle					
CACC System	23.94%	31.12%	38.1%	43.83%	48.45%
Gap-regulating Mode Ratio	57.39%	56.39%	52.47%	48.03%	45.55%
Number of Deactivations per CACC vehicle					
Total	5.86	6.06	4.66	3.32	3.43
Lane-change related	2.25	2.35	2.05	1.65	1.71
Safety-related	2.97	3.05	1.93	1.01	1.06
Route-related	0.64	0.66	0.68	0.67	0.66

FIG 7 Mean and standard deviation of the travel time delay of conventional and CACC vehicles at each CACC MPRs.

MPRs as the CACC MPR increases, mainly because traffic congestion was mitigated with increasing CACC vehicles and less collision warning is issued thereof. The lane-

change-related deactivation decreases at 40% and 50% CACC MPRs as well. This can be explained by the fact that the traffic performance in CACC lane is not significantly better than the GP lanes and fewer lane changes are made by CACC vehicles toward the CACC lanes and fewer cooperative maneuvers are needed.

V. Conclusion and Future Work

This study was designed to investigate the quantitative impacts of converting an HOV lane to a CACC dedicated lane on traffic flow, travel time and CACC string operation at low and medium CACC MPRs. Based on an enhanced car-following model for CACC vehicles and an extended lane change model for a dedicated lane scenario, we conducted microscopic simulations to reproduce the traffic flows with mixed CACC vehicles and manually driven vehicles with a leftmost CACC dedicated lane on a freeway corridor in California. The simulation results were compared to a reference case with an HOV lane and the comparison revealed the positive and negative impacts of CACC lanes in terms of traffic flow performance.

This study showed that converting an HOV lane to a CACC dedicated lane has different impacts depending on the market penetration rate of CACC vehicles. The results of 30% CACC MPR with a CACC lane is comparable to the reference case of an HOV lane which has around 29% HOVs during the congestion formation. At CACC MPRs below 30%, the CACC lane carries insufficient traffic and the GP lanes bear a higher demand than the reference case, which causes severe and long-lasting traffic congestion. The total travel time substantially increases and the travel time reliability decreases. However, at CACC MPRs ranging from 30%–50%, the traffic congestion are considerably alleviated by a high lane flow share of the CACC lane and the CACC operation in GP lanes. In these cases, the travel time and delay dramatically decrease and the travel time reliability increases. At low CACC MPRs where congestions happen, this study also found that a CACC lane can provide smaller travel time delay and higher travel time reliability to CACC vehicles than that of the manually driven vehicles in GP lanes. In terms of CACC operations in a CACC lane scenario, the CACC time usage is found to be increasing with the CACC MPR, but the time of CACC operations under gap-regulating mode is found to be decreasing as the CACC MPR increases.

The findings of this research provide new insights into the effects and operation of a CACC dedicated lane. An important implication to road operator is that the conversion from an existing HOV lane to a CACC lane should wait until the CACC MPR has risen to a certain level. Otherwise, the overall traffic can deteriorate due to a closed lane for manually driven vehicles. Mixed use of dedicated lanes at low CACC MPRs is likely to be a transitional strategy before reaching sufficient CACC demand, which is in accordance with the literature. As the CACC vehicle information could be used for traffic state estimation at a lane level [38], [39], road operator may also consider to dynamically activate/deactivate CACC dedicated lanes depending on the estimated traffic states.

The results of the friction effect between CACC lanes and GP lanes also raise a safety concern: at low CACC MPRs, the large speed difference between two lanes can result in high collision risk when a lane change is performed. Especially when CACC systems are activated, drivers pay less attention to surrounding vehicles, and they may not respond in time to resume vehicle controls and avoid collisions. To reduce the collision risks, communication and coordination between lane changing vehicles and vehicles in CACC lanes are essential. A future study will focus on strategies to increase the flow of CACC lanes as the CACC MRP is low, for instance, by allowing connected (conventional) vehicles to act as string leader and use CACC dedicated lanes. In addition, future research may pay attention to the save in travel time by CACC vehicles with different travel distance. It may provide a detailed quantitative analysis of CACC system usage for different CACC users. Moreover, future work may investigate the scenario of increasing CACC vehicles in a highway with an activated HOV lane, as the intermediate phase of converting an HOV lane to a CACC lane.

About the Authors

Lin Xiao received the M.Sc. degree in Transportation Planning and Management from Tongji University, China in 2013. She is currently working as a Ph.D. researcher in the Department of Transport & Planning at Delft University of Technology, the Netherlands. Her research interests include the modelling of automated vehicles in microscopic traffic simulations and the impacts of automated vehicles on traffic flow performance.

Meng Wang (M'15) received the B.Sc. in Civil Engineering at Tsinghua University, M.Sc. degree in Transportation Engineering at Research Institute of Highway and Ph.D. degree with distinction at Delft University of Technology, the Netherlands, in 2006 and 2014

respectively. He worked as researcher in National ITS Engineering Centre, China from 2006 to 2009. From 2014 to 2015, he worked as Postdoctoral Researcher at the Department of BioMechanical Engineering at TU Delft. From 2015 onwards, he works as Assistant Professor at the Department of Transport & Planning, TU Delft. He is Co-Director of the hEAT lab (Research Lab on Electric and Automated Transport). His main research interests are decision-making and control design of cooperative driving systems and traffic flow impact assessment of such systems.

Bart van Arem (M'04–SM'16) received the M.S. and Ph.D. degrees in applied mathematics and speciality queuing theory from the University of Twente, Enschede, The Netherlands, in 1986 and 1990, respectively. From 1992 and 2009, he was a Researcher and Program Manager with TNO, working on intelligent transport systems, in which he has been active in various national and international projects. Since 2009, he has been a Full Professor of Intelligent Transport Modelling with the Department of Transport and Planning, Faculty of Civil Engineering and Geosciences, Delft University of Technology, Delft, The Netherlands. His research focuses on modelling the impact of intelligent transport systems on mobility.

References

[1] R. Hoogendoorn, B. van Arem, and S. Hoogendoorn, "Automated driving, traffic flow efficiency, and human factors," *Transp. Res. Record, J. Transport. Res. Board*, vol. 2422, pp. 113–120, 2014. doi: 10.3141/2422-13.

[2] S. E. Shladover, C. Nowakowski, X. Y. Lu, and R. Ferlis, "Cooperative adaptive cruise control: Definitions and operating concepts," *Transp. Res. Record, J. Transport. Res. Board*, vol. 2489, pp. 145–152, 2015. doi: 10.3141/2489-17.

[3] D. Swaroop, J. K. Hedrick, C. C. Chien, and P. Ioannou, "A comparison of spacing and headway control laws for automatically controlled vehicles," *Veh. Syst. Dyn., Int. J. Veh. Mech. Mobil.*, vol. 23, no. 1, pp. 597–625, 1994. doi: 10.1080/00423119408969077.

[4] A. Kanaris, P. Ioannou, and F. S. Ho, "Spacing and capacity evaluations for different AHS concepts," in *Proc. 1997 American Control Conf.*, Albuquerque, NM, 1997, pp. 2056–2040.

[5] J. B. Michael, D. N. Godbole, J. Lygeros, and R. Sengupta, "Capacity analysis of traffic flow over a single-lane automated highway system," *ITS J., Intell. Transp. Syst. J.*, vol. 4, nos. 1–2, pp. 49–80, 1998. doi: 10.1080/10248079808903736.

[6] R. W. Hall and C. Li, "Lane capacity for an automated highway with mixed vehicle classes," *ITS J., Intell. Transp. Syst. J.*, vol. 5, no. 3, pp. 217–240, 1999. doi: 10.1080/10248079908903767.

[7] A. I. Delis, I. K. Nikolos, and M. Papageorgiou, "Simulation of the penetration rate effects of ACC and CACC on macroscopic traffic dynamics," presented at the 19th Int. Conf. Intelligent Transportation Systems (ITSC), Rio de Janeiro, 2016.

[8] I. K. Nikolos, A. I. Delis, and M. Papageorgiou, "Macroscopic modelling and simulation of ACC and CACC traffic," presented at the 18th Int. Conf. Intelligent Transportation Systems (ITSC), Las Palmas, 2015.

[9] D. Ngoduy, "Instability of cooperative adaptive cruise control traffic flow: A macroscopic approach," *Commun. Nonlinear Sci. Numer. Simul.*, vol. 18, no. 10, pp. 2838–2851, 2013. doi: 10.1016/j.cnsns.2013.02.007.

[10] S. E. Shladover, D. Su, and X.-Y. Lu, "Impacts of cooperative adaptive cruise control on freeway traffic flow," *Transp. Res. Record, J. Transport. Res. Board*, vol. 2324, pp. 63–70, 2012. doi: 10.3141/2324-08.

[11] J. VanderWerf, S. E. Shladover, M. A. Miller, and N. Kourjanskaia, "Effects of adaptive cruise control systems on highway traffic flow capacity," *Transp. Res. Record, J. Transport. Res. Board*, vol. 1800, pp. 78–84, 2002. doi: 10.3141/1800-10.

[12] L. Zhao and J. Sun, "Simulation framework for vehicle platooning and car-following behaviors under connected-vehicle environment," *Proced., Soc. Behav. Sci.*, vol. 96, pp. 914–924, 2013. doi: 10.1016/j.sbspro.2013.08.105.

[13] A. Talebpour and H. S. Mahmassani, "Influence of connected and autonomous vehicles on traffic flow stability and throughput," *Transp. Res. C, Emerg. Technol.*, vol. 71, pp. 143–163, 2016. doi: 10.1016/j.trc.2016.07.007.

[14] M. Hartmann, N. Motamedidehkordi, S. Krause, S. Hoffmann, P. Vortisch, and F. Busch, "Impact of automated vehicles on capacity of the German freeway network," presented at the ITS World Congress, Montreal, Canada, 2017.

[15] G. M. Arnaout and J. P. Arnaout, "Exploring the effects of cooperative adaptive cruise control on highway traffic flow using microscopic traffic simulation," *Transp. Plan. Technol.*, vol. 37, no. 2, pp. 186–199, 2014. doi: 10.1080/03081060.2013.870791.

[16] B. van Arem, C. J. G. van Driel, and R. Visser, "The impact of cooperative adaptive cruise control on traffic-flow characteristics," *IEEE Trans. Intell. Transp. Syst.*, vol. 7, no. 4, pp. 429–436, 2006. doi: 10.1109/TITS.2006.884615.

[17] M. Makridis, K. Mattas, B. Ciuffo, M. A. Raposo, and C. Thiel, "Assessing the impact of connected and automated vehicles. A freeway scenario," in *Advanced Microsystems for Automotive Applications.* New York: Springer-Verlag, 2017, pp. 213–225.

[18] L. Xiao, M. Wang, W. Schakel, and B. van Arem, "Unravelling effects of cooperative adaptive cruise control deactivation on traffic flow characteristics at merging bottlenecks," *Transp. Res. C, Emerg. Technol.*, vol. 96, pp. 380–397, 2018. doi: 10.1016/j.trc.2018.10.008.

[19] A. Talebpour, H. S. Mahmassani, and A. Elfar, "Investigating the effects of reserved lanes for autonomous vehicles on congestion and travel time reliability," *Transp. Res. Record, J. Transport. Res. Board*, vol. 2622, pp. 1–12, 2017. doi: 10.3141/2622-01.

[20] H. Liu, X. Kan, S. E. Shladover, X.-Y. Lu, and R. E. Ferlis, "Modeling impacts of cooperative adaptive cruise control on mixed traffic flow in multi-lane freeway facilities," *Transp. Res. C, Emerg. Technol.*, vol. 95, pp. 261–279, 2018. doi: 10.1016/j.trc.2018.07.027.

[21] Z. B. Chen, F. He, L. H. Zhang, and Y. F. Yin, "Optimal deployment of autonomous vehicle lanes with endogenous market penetration," *Transp. Res. C, Emerg. Technol.*, vol. 72, pp. 143–156, 2016. doi: 10.1016/j.trc.2016.09.013.

[22] G. M. Arnaout and S. Bowling, "A progressive deployment strategy for cooperative adaptive cruise control to improve traffic dynamics," *Int. J. Autom. Comput.*, vol. 11, no. 1, pp. 10–18, 2014. doi: 10.1007/s11633-014-0760-2.

[23] S. F. Qom, Y. Xiao, and M. Hadi, "Evaluation of cooperative adaptive cruise control (CACC) vehicles on managed lanes utilizing macroscopic and mesoscopic simulation," in *Proc. Transportation Research Board 95th Annu. Meeting*, Washington, D.C., 2016.

[24] D. J. Chen, S. Ahn, M. Chitturi, and D. A. Noyce, "Towards vehicle automation: Roadway capacity formulation for traffic mixed with regular and automated vehicles," *Transp. Res. B, Methodol.*, vol. 100, pp. 196–221, 2017. doi: 10.1016/j.trb.2017.01.017.

[25] L. Xiao, M. Wang, W. J. Schakel, S. E. Shladover, and B. van Arem, "Modeling lane change behavior on a highway with a high occupancy vehicle lane with continuous access and egress," in *Proc. Transportation Research Board 96th Annu. Meeting*, Washington, D.C., 2017.

[26] L. Xiao, M. Wang, and B. van Arem, "Realistic car-following models for microscopic simulation of adaptive and cooperative adaptive cruise control vehicles," *Transp. Res. Record, J. Transport. Res. Board*, vol. 2623, pp. 1–9, 2017. doi: 10.3141/2623-01.

[27] V. Milanés and S. E. Shladover, "Handling cut-in vehicles in strings of cooperative adaptive cruise control vehicles," *J. Intell. Transp. Syst.*, vol. 20, no. 2, pp. 178–191, 2015. doi: 10.1080/15472450.2015.1016023.

[28] V. Milanés, S. E. Shladover, J. Spring, C. Nowakowski, H. Kawazoe, and M. Nakamura, "Cooperative adaptive cruise control in real traffic situations," *IEEE Trans. Intell. Transp. Syst.*, vol. 15, no. 1, pp. 296–305, 2014. doi: 10.1109/TITS.2013.2278494.

[29] V. Milanés and S. E. Shladover, "Modeling cooperative and autonomous adaptive cruise control dynamic responses using experimental data," *Transp. Res. C, Emerg. Technol.*, vol. 48, pp. 285–300, 2014. doi: 10.1016/j.trc.2014.09.001.

[30] C. Nowakowski et al., "Cooperative adaptive cruise control: Testing drivers' choices of following distances," California PATH Research Report, Berkeley, CA, UCB-ITS-PRR-2011-01, 2011.

[31] H. Liu, X. Kan, S. E. Shladover, X.-Y. Lu, and R. E. Ferlis, "Impact of cooperative adaptive cruise control on multilane freeway merge capacity," *J. Intell. Transp. Syst.*, vol. 22, no. 3, pp. 263–275, 2018. doi: 10.1080/15472450.2018.1438275.

[32] R. J. Kiefer, D. J. LeBlanc, and C. A. Flannagan, "Developing an inverse time-to-collision crash alert timing approach based on drivers' last-second braking and steering judgments," *Accid. Anal. Prev.*, vol. 37, no. 2, pp. 295–303, 2005. doi: 10.1016/j.aap.2004.09.003.

[33] M. Treiber, A. Hennecke, and D. Helbing, "Congested traffic states in empirical observations and microscopic simulations," *Phys. Rev. E*, vol. 62, no. 2, pp. 1805–1824, 2000. doi: 10.1103/PhysRevE.62.1805.

[34] W. J. Schakel, B. van Arem, and B. D. Netten, "Effects of cooperative adaptive cruise control on traffic flow stability," in *Proc. the 13th Int. IEEE Annu. Conf. Intelligent Transportation Systems*, Madeira Island, Portugal, 2010, pp. 759–764.

[35] W. J. Schakel, V. L. Knoop, and B. van Arem, "Integrated lane change model with relaxation and synchronization," *Transp. Res. Record, J. Transport. Res. Board*, vol. 2316, pp. 47–57, 2012. doi: 10.3141/2316-06.

[36] W. J. Schakel, "MOTUS." [Online]. Available: http://homepage.tudelft.nl/05a3n/

[37] A. Guin, M. Hunter, and R. Guensler, "Analysis of reduction in effective capacities of high-occupancy vehicle lanes related to traffic behavior," *Transp. Res. Record, J. Transport. Res. Board*, vol. 2065, pp. 47–53, 2008. doi: 10.3141/2065-07.

[38] M. Fountoulakis, N. Bekiaris-Liberis, C. Roncoli, I. Papamichail, and M. Papageorgiou, "Highway traffic state estimation with mixed connected and conventional vehicles: Microscopic simulation-based testing," *Transp. Res. C, Emerg. Technol.*, vol. 78, pp. 13–33, 2017. doi: 10.1016/j.trc.2017.02.015.

[39] S. Papadopoulou, C. Roncoli, N. Bekiaris-Liberis, I. Papamichail, and M. Papageorgiou, "Microscopic simulation-based validation of a per-lane traffic state estimation scheme for highways with connected vehicles," *Transp. Res. C, Emerg. Technol.*, vol. 86, pp. 441–452, 2018. doi: 10.1016/j.trc.2017.11.012.

ITS